Magnetostriction and magnetoelastic domains in antiferromagnets

2002 J. Phys.: Condens. Matter 14 3959

(http://iopscience.iop.org/0953-8984/14/15/310)

INSTITUTE OF PHYSICS PUBLISHING JOURNAL OF PHYSICS: CONDENSED MATTER

J. Phys.: Condens. Matter **14** (2002) 3959–3971 PII: S0953-8984(02)20614-1

Magnetostriction and magnetoelastic domains in antiferromagnets

Helen Gomonay[1,2] **and Vadim M Loktev**[1]

[1] National Technical University of Ukraine 'KPI', 37, ave. Peremogy, 03056, Kiev, Ukraine
[2] Max Planck Institute of Microstructure Physics, Weinberg 2, D-06120, Halle, Germany

E-mail: malyshen@ukrpack.net

Received 9 January 2001, in final form 12 December 2001
Published 4 April 2002
Online at stacks.iop.org/JPhysCM/14/3959

Abstract

The problem of the observable equilibrium domain structure (DS) in pure antiferromagnets is investigated with the use of continuous elasticity theory. It is shown that the difference between the bulk and surface magnetoelastic strains causes imaginary 'incompatibility elastic charges' analogous to the surface 'magnetic' charges in ferromagnets. The corresponding long-range field is shown to contribute to the 'stray' energy of the sample that governs the appearance of the DS, the contribution from the 'elastic charges' being proportional to the sample volume. Competition between the elastic 'stray' field, which favours inhomogeneous strain distribution, and an external field, which tends to make the sample homogeneous, provides a reversible reconstruction of the DS under the action of the external magnetic field.

1. Introduction

The idea of antiferromagnetic domains was suggested by Néel [1] nearly 50 years ago to explain the behaviour of the susceptibility of antiferromagnets (AFM) in external magnetic fields. Since that time, numerous experiments have confirmed the existence of domains in such AFM as NiO [2–4], CoO [5, 6], $CoCl_2$ [7], CoF_2 [8], $YBa_2Cu_3O_{6+x}$ [9, 10], Cr [11], UPdSn [12], and MnTe [13], despite the difficulties in directly observing them. The experiments show not only the presence of domain structure (DS), but also its redistribution under the action of an external magnetic field or mechanical stress and reappearance after the field is removed. Such stability and reversible behaviour of the DS in AFM, which undoubtedly reveals their thermodynamic origin, is still not explained. While formation of domains in ferromagnets is promoted by the reduction of magnetostatic energy, the AFM possess no local magnetization in the absence of an external field and there seems to be no obvious counterbalance to the increase of the free energy produced by the domain walls. Most of the theoretical papers in this field (see, e.g., [14–16]) deal with weak ferromagnets with small but non-zero non-compensated local magnetization or take the AFM DS as an *artefact*. Usually, the formation of the domains in

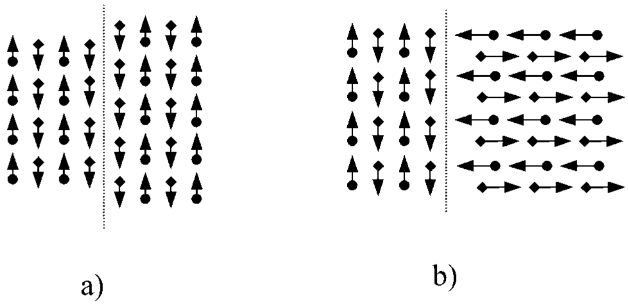

Figure 1. Translational (*a*) and orientational (*b*) AFM domains. Arrows show orientations of spins at each site.

AFM is related to local fluctuations of the AFM order at the Néel temperature with subsequent pinning of the domain walls by lattice imperfections. Li [17] has attributed the stability of the DS to the interplay between the wall energy and a gain in entropy of the walls, but his estimates show that the entropy contribution to the free energy is much too small to compensate for the wall energy.

In general, there are two types of domain in AFM—so-called translational, or collinear, domains with an antiparallel orientation of the magnetic vectors in the neighbouring domains (and separated by a change-of-step boundary, according to the Li [17] classification) and orientational domains, for which the magnetic axes in different domains are non-collinear (separated by a change-of-axis boundary). In the former case, sketched in figure 1(*a*), the AFM domains cannot be physically distinguished unless there is an additional source of contrast, such as the different environments of the magnetic atoms in MnF_2 and CoF_2 investigated in [8, 18, 19], along with other exotic AFM. The latter case (figure 1(*b*)) is typical for crystals which possess several crystallographically equivalent directions for the AFM vectors and where corresponding magnetic domains can be associated with crystallographic twins.

A peculiar feature of the orientational AFM domains is that they show different spontaneous strains and lattice distortions. In fact, this makes it possible to observe the AFM domains by the x-ray topographic technique and facilitates optical observations due to the contrast enhancement. The magnetoelastic nature of the orientational AFM domains, claimed by Tanner and Safa [20, 21] and experimentally proven in [2, 16, 22–24], opens up the possibility of applying the approaches developed for the description of the transition-induced microstructure in crystals that undergo a martensitic-like phase transition. The martensitic phase transition is a diffusionless transition associated with a finite displacement of the atoms in the unit cell. This transition usually has first-order nature and proceeds through the motion of coherent interfaces. In the absence of external fields the product phase is twinned; the twinned regions take the form of plane-parallel stripes with flat interfaces. The main feature of the martensitic phase transition is that it is usually followed by the appearance of rather large (up to 5–10%) spontaneous strains. In other words, temperature variation produces a kind of ‘plastic’ deformation which, as was pointed out by Olson and Cohen [25], differs from the intrinsically unstable states associated with an elastic deformation. Formation of the domain (twin) structure in this case is caused by incompatibility of lattice deformation between the parent and martensitic phase at the internal interfaces (figure 2). Such a lattice-invariant deformation produces a change of shape and reduces macroscopic stresses. Mechanical twinning can also reduce macroscopic stresses which arise due to lattice misfit in polysynthetic structures [26]. So, an interface produces a kind of restoring force which tends to conserve the shape of the martensitic phase and gives rise to equilibrium DS.

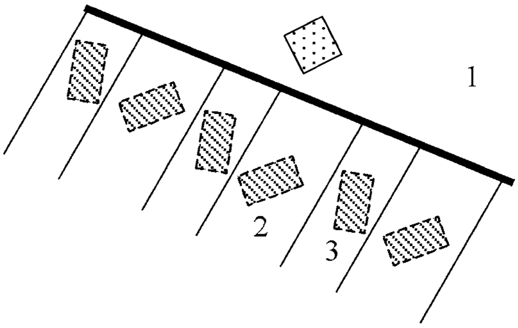

Figure 2. Formation of the twin structure in martensite. The square in region 1 is a sketch of a unit cell of the parent phase, and rectangles 2, 3 represent unit cells in the deformed martensite region.

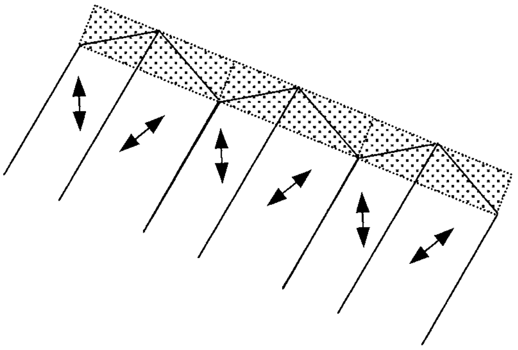

Figure 3. Incompatibility: continuity in the near-surface region (shaded) is locally corrupted below the Néel point; it can be restored on average by twin formation. Arrows sketch the easy axes for the AFM vectors.

On the other hand, martensites and AFM differ not only in the value of the spontaneous strain (which for martensites is usually 1–2 orders of magnitude greater than for AFM), but also in the absence of the internal transformation-induced interfaces in AFM. In the present paper we argue that a sample surface, like an interface in the martensites, may be a source of a 'restoring force' in AFM and can cause formation of an equilibrium DS. We also develop a model which takes a broader view of our previous results [27, 28] and allows us to describe the recent observations [24, 29–33] of the macroscopic properties of AFM in external magnetic fields.

2. 'Stray' energy

Due to the abrupt change in the atomic surroundings, a surface has properties which are strongly or sometimes crucially different from those of the bulk. This distinction is intensified in the course of a phase transition. For example, in AFM crystals a long-range magnetic order in the bulk of the sample is preserved at substantially higher temperature than at the surface [34–36]. In addition, wide-ranging experimental findings concerning the elastic and magnetoelastic properties of thin films and multilayers (see, e.g., [37–39]) make it possible to assume that the elastic properties of the surface are also quite different. Thus, a surface could be considered as a phase tightly bonded with the bulk, with its own elastic, magnetic, and other characteristics.

Suppose that a sample goes through the Néel temperature. The AFM vectors which occur in the bulk try to produce the spontaneous quasi-plastic strains $\hat{u}^{(0)}(\boldsymbol{r})$ which would appear locally in the case of homogeneous distribution. The more inert (with respect to appearance of magnetization) surface is described by a different strain tensor $\hat{u}^{(S)}$. The strain incompatibilities that appear produce internal mechanical stresses that must be relaxed by additional elastic strains $\hat{u}^{+}(\boldsymbol{r})$, so the total strain with respect to the reference state is

$$\hat{u}_{\text{total}} = \hat{u}^{(0)} + \hat{u}^{+}(\boldsymbol{r}), \tag{1}$$

and represents a compatible state of deformation. In the case where the distribution of the AFM vectors in the intermediate region between the bulk and surface does not play a significant role, we can introduce an incompatibility tensor $\hat{\eta}$ as follows:

$$\eta_{ip}(\boldsymbol{r}) = -\varepsilon_{ikl}\varepsilon_{pmt} n_k^{(S)} [u_{lt}^{(0)} - u_{lt}^{(S)}] n_m^{(S)} \delta\prime[\boldsymbol{n}^{(S)}(\boldsymbol{r} - \boldsymbol{r}_S)], \tag{2}$$

where ε_{ikl} is the antisymmetric Levi-Civita permutation tensor and $\boldsymbol{n}^{(S)}$ is a vector normal to the sample surface. Defined as a Dirac delta-function, δ is non-zero in the close vicinity of the surface; the prime means the derivative with respect to the argument. In what follows we will set the surface strain to zero, $\hat{u}^{(S)} = 0$. This simplest approximation is applicable to the temperature interval below the Néel point in which the surface is still non-magnetic and to systems with small surface magnetoelastic coupling or non-softening elastic moduli. The more general case of non-zero surface strains can be treated in an analogous way.

The incompatibility $\hat{\eta}$ can be considered as a result of the presence of fictitious dislocations with infinitesimal Burgers vectors continuously distributed at the surface. This concept of magnetically induced quasi-dislocations was developed by Kléman [40] for the domain walls inside ferromagnets. Then, we can apply Eshelby's approach [41] for calculation of the additional dislocation-induced strains $\hat{u}^{+}(\boldsymbol{r})$. According to standard elasticity theory, the function $\hat{u}^{+}(\boldsymbol{r})$ must satisfy the equations

$$\varepsilon_{ikl}\varepsilon_{pmt}\frac{\partial^2 u_{km}^{+}}{\partial x_l\,\partial x_t} = \eta_{ip}, \tag{3}$$

$$\operatorname{div}\hat{\sigma}^{+} \equiv \frac{\partial \sigma_{ij}^{+}}{\partial x_j} = \boldsymbol{f}_V, \tag{4}$$

with boundary conditions for the relaxed stresses at the sample surface:

$$\hat{\sigma}^{+}\boldsymbol{n}^{(S)} = \boldsymbol{f}^{(S)}. \tag{5}$$

In equation (4) the stresses $\hat{\sigma}^{+}$ are related to the additional strains $\hat{u}^{+}$ by Hooke's law. The vectors $\boldsymbol{f}_V$ and $\boldsymbol{f}^{(S)}$ describe, respectively, the bulk forces and surface loads produced by dislocations. Eshelby proposed calculating them as

$$\boldsymbol{f}_V = -\operatorname{div}\hat{\hat{c}}\hat{u}_{\text{par}}, \qquad \boldsymbol{f}^{(S)} = -\boldsymbol{n}^{(S)}\hat{\hat{c}}\hat{u}_{\text{par}}, \tag{6}$$

where $\hat{u}_{\text{par}}$ is a particular solution of equation (3):

$$\hat{u}_{\text{par}}(\boldsymbol{r}) = \frac{1}{4\pi}\int_V \mathrm{d}\boldsymbol{r}_1 \,\frac{\hat{\eta}(\boldsymbol{r}_1) - \hat{1}\,\mathrm{Tr}\,\hat{\eta}(\boldsymbol{r}_1)}{|\boldsymbol{r} - \boldsymbol{r}_1|}, \tag{7}$$

and $\hat{\hat{c}}$ is a tensor of the bulk elastic moduli.

In the case of quasi-dislocations located mainly at the sample surface, we can express $\hat{u}_{\text{par}}$ as

$$\hat{u}_{\text{par}}(\boldsymbol{r}) = \frac{1}{4\pi}\int_S \mathrm{d}S\,\frac{(\boldsymbol{n}, \boldsymbol{r} - \boldsymbol{r}_S)}{|\boldsymbol{r} - \boldsymbol{r}_S|^3}\hat{\boldsymbol{U}}(\boldsymbol{r}_S) = -\frac{1}{4\pi}\int \mathrm{d}\Omega_r\,\hat{\boldsymbol{U}}(\boldsymbol{r}_S), \tag{8}$$

where $\mathrm{d}\Omega_r$ is an increment of solid angle at which the surface point $\boldsymbol{r}_S$ is seen from the given point $\boldsymbol{r}$. The expression for the tensor

$$\hat{\boldsymbol{U}}(\boldsymbol{r}_S) \equiv \hat{u}^{(0)}(\boldsymbol{r}_S) + \boldsymbol{n}^{(S)} \otimes \boldsymbol{n}^{(S)} \,\mathrm{Tr}\, \hat{u}^{(0)}(\boldsymbol{r}_S) - \boldsymbol{n}^{(S)} \otimes (\hat{u}^{(0)}(\boldsymbol{r}_S)\boldsymbol{n}^{(S)}) - (\hat{u}^{(0)}(\boldsymbol{r}_S)\boldsymbol{n}^{(S)}) \otimes \boldsymbol{n}^{(S)} \tag{9}$$

includes only those combinations of the spontaneous strain tensor $\hat{u}^{(0)}$ which are tangential to the surface at a given point $\boldsymbol{r}_S$. They can be treated as a tensor of additional deformations that compensate for the incompatibility between the surface and the bulk strains or, by analogy with the physics of magnetism, as a tensor of ‘elastic charges’ located at the surface.

For practical applications it is more convenient to use a variational method in which an optimum strain distribution corresponds to the minimum of a functional:

$$\Phi = \int_V f_{\mathrm{bulk}}(\boldsymbol{r})\,\mathrm{d}\boldsymbol{r} + F_{\mathrm{stray}} + F_{\mathrm{surf}}, \tag{10}$$

which, by analogy with magnetostatics, comprises the shape-dependent stray energy of ‘elastic charges’:

$$F_{\mathrm{stray}} = \frac{1}{4\pi}\int_V \mathrm{d}\boldsymbol{r} \int_S \mathrm{d}\Omega_r\, \hat{u}^{+}(\boldsymbol{r})\hat{\hat{c}}\hat{\boldsymbol{U}}(\boldsymbol{r}_S), \tag{11}$$

where $\hat{\boldsymbol{U}}(\boldsymbol{r}_S)$ is defined in (9).

It can easily be verified that the expressions (4), (5) are Euler-type equations for the functional (10).

In equation (10) we have also taken account of a free-energy density f_{bulk} of the sample which may include elastic as well as magnetic contributions. The last term, given by the equation

$$F_{\mathrm{surf}} = \int \mathrm{d}S\,[\alpha_S + \hat{\beta}_S\hat{u}_S(\boldsymbol{r}_S) + \tfrac{1}{2}\hat{u}_S(\boldsymbol{r}_S)\hat{\hat{c}}_S\hat{u}_S(\boldsymbol{r}_S)], \tag{12}$$

describes the surface energy [42]. Coefficients α_S and $\hat{\beta}_S$ characterize the surface tension; $\hat{\hat{c}}_S$ is the tensor of the surface elastic moduli. In the general case, $\hat{\hat{c}}_S$ is different from the corresponding bulk tensor, and the surface strain tensor $\hat{u}_S(\boldsymbol{r}_S)$ is supposed to have only tangential components. The surface energy (12) defines equilibrium surface strains below the Néel point and it is also important for the setting up of the equilibrium shape of the sample (it establishes the minimum surface area at a given volume). In the approximation considered ($\hat{u}_S = 0$), the surface elastic moduli are supposed to be much greater than those of a bulk (formally, $\hat{\hat{c}}_S \to \infty$).

3. Equilibrium domain structure

The inhomogeneous equilibrium state of AFM may be found by minimizing the functional (10) with respect to the independent magnetization components and elastic displacements. Without preliminary information about the features of the DS, this problem becomes very complicated, especially for the cases treating rearrangement of the domains under the action of external fields. Additional complication as compared e.g. to the ferromagnets case arises from three-dimensional non-locality and tensor character of the elastic ‘charges’ and fields. Substantial simplification can be achieved if we assume that the characteristic length of the DS is much smaller than the size of the sample. In this case the main contribution to the stray energy arises from macrostresses:

$$\langle\hat{\sigma}_{\mathrm{macro}}\rangle = \frac{1}{V}\int \mathrm{d}V\,\hat{\hat{c}}\hat{u}_{\mathrm{par}} \tag{13}$$

related to the averaged spontaneous strains

$$\langle \hat{u}^{(0)} \rangle = \frac{1}{V} \int_V \mathrm{d}\boldsymbol{r}\, \hat{u}^{(0)}(\boldsymbol{r}). \tag{14}$$

Further calculations require an outline of the sample shape. For a typical case of a $\boldsymbol{n}_S$-oriented thin plate, $\hat{u}_{\mathrm{par}}$ is homogeneous and, according to (6), $\boldsymbol{f}_V = 0$. An obvious solution of equations (4) and (5) is $\hat{u}^+ = -\langle \hat{u}_{\mathrm{par}} \rangle$ and the stray energy of the macrostresses (13) takes the form

$$\begin{aligned} F_{\mathrm{stray}} &= L^2 d \langle \hat{\boldsymbol{U}} \rangle \hat{\hat{c}} \langle \hat{\boldsymbol{U}} \rangle, \\ \langle \hat{\boldsymbol{U}} \rangle &\equiv \langle \hat{u}^{(0)} \rangle + \boldsymbol{n}_S \otimes \boldsymbol{n}_S \,\mathrm{Tr} \langle \hat{u}^{(0)} \rangle - \boldsymbol{n}_S \otimes (\langle \hat{u}^{(0)} \rangle \boldsymbol{n}_S) - (\langle \hat{u}^{(0)} \rangle \boldsymbol{n}_S) \otimes \boldsymbol{n}_S. \end{aligned} \tag{15}$$

In (15) d is the thickness of the plate, which is much less than its transverse size L. It is also evident from relation (15) that the stray energy is non-negative, $F_{\mathrm{stray}} \geqslant 0$, and in the absence of an external field it can only be reduced by zeroing of the average strains.

The value of F_{stray} (15) depends upon the shape of the sample. In our case, it depends on the orientation of the surface normal with respect to the crystallographic axes. If the surface normal $\boldsymbol{n}_S$ is oriented along the principal symmetry axis C_n of the sample ($n = 3, 4$, or 6), then the macroscopic symmetry of the sample coincides with the crystallographic symmetry and must be restored below the phase transition point by formation of the DS (in accordance with the Curie principle which states that the tensor characteristic of the cause must coincide with the tensor characteristic of the effect; thus, the temperature which causes the AFM transition may produce on average only a scalar effect). So, all the types of domain should be equally represented.

The above calculations show convincingly that the appearance of the homogeneous deviatoric (shear) strains in the finite-size sample can give rise to a considerable energy increase and thus is not advantageous. There is a close analogy between the appearance of the long-range elastic fields in thermoelastics and dipole fields in ferromagnets (a similarity between the equations for electromagnetic fields in substances and equations of elasticity theory was noticed by de Wit long ago [43]). The case of weak ferromagnets needs special treatment because the DS in corresponding compounds can be formed due to competition of demagnetization and twinning factors. However, this problem is beyond the scope of this paper.

To continue the analogy with the problem of ferromagnetic domains, we should emphasize some properties of the stray (twinning) field. First, the energy contribution resulting from the 'incompatibility charges' located at the surface (see (15)) is proportional to the sample volume V and thus, in principle, is independent of sample size. Second, the additional strain field (8) is scaling invariant. In other words, the additional strain distribution inside the sample depends only upon the angle at which the surface is seen from a given point. So, isomorphic transformation of the sample does not change the additional strain distribution.

From the above arguments we can draw a rather general conclusion: in the case of a temperature-induced phase transition the macroscopic symmetries of the sample in low- and high-temperature phases are the same. If the transition is symmetry breaking (on the microscopic scale), i.e. the microscopic order parameter is conjugated with non-isomorphous striction and produces strains that locally reduce the symmetry of the crystal lattice, then macroscopic symmetry is restored due to the onset of the DS with differently oriented strain tensors. In the general case, the macroscopic symmetry of the sample can be lower than the crystallographic one due to previous treatment of the sample, experimental conditions, mechanical load, etc. In this case the DS of the AFM phase may contain more domains of a certain type or may even be single domain.

Another important question that arises while analysing expression (10) is that of whether the onset of twin (domain) structure is indeed thermodynamically advantageous. The point is that the inhomogeneous strain distribution gives rise to an increase of the full free energy due to the contribution of the domain walls. In order to show that the stray-energy gain is greater than the loss from the domain wall contribution, let us follow the method applied to ferromagnets and consider the DS consisting of two alternating types of domain, characterized with the strain tensors $\hat{u}_1$ and $\hat{u}_2$; the period of the DS d_{DS} is much smaller than the plate thickness, $d_{\mathrm{DS}} \ll d$. Different domains produce 'charges' of opposite signs. In the near-surface region, at distances of the order of d_{DS} (in accordance with the empirical St Venan principle), the corresponding stress field is not compensated and it contributes to the free energy as follows:

$$F_{\mathrm{ch}} = L^2 d_{\mathrm{DS}} \xi_1 \xi_2 (\hat{u}_1 - \hat{u}_2)\hat{\hat{c}}(\hat{u}_1 - \hat{u}_2)\cos\vartheta, \tag{16}$$

where ϑ is the angle between the plate surface and the domain (twin) interface, ξ_1 $(=1-\xi_2)$ is the volume fraction of the domain of the first type.

Domain walls (interfaces) also contribute to the free energy:

$$F_{\mathrm{DW}} = L^2 \sigma_{\mathrm{DW}} \frac{d}{d_{\mathrm{DS}}}, \tag{17}$$

where σ_{DW} is the surface energy of a single domain wall.

Comparison of the above equations shows that the energy of the domain walls (17) competes with the short-range contribution from the 'elastic charges' (16) and thus defines an equilibrium DS period:

$$d_{\mathrm{DS}}^{\mathrm{opt}} = \frac{\sqrt{\sigma_{\mathrm{DW}} d}}{\sqrt{\xi_1 \xi_2 (\hat{u}_1 - \hat{u}_2)\hat{\hat{c}}(\hat{u}_1 - \hat{u}_2)\cos\vartheta}} \simeq \sqrt{\frac{\sigma_{\mathrm{DW}} d}{F_{\mathrm{el}}}}. \tag{18}$$

So, the contribution from the inhomogeneous part of the strains and the short-range periodic 'charge' distribution,

$$F_{\mathrm{inh}} \propto F_{\mathrm{DW}}(d_{\mathrm{DS}}^{\mathrm{opt}}) \propto V(\hat{u}^{(0)}\hat{\hat{c}}\hat{u}^{(0)})\frac{d_{\mathrm{DS}}}{d} \propto F_{\mathrm{stray}}\frac{d_{\mathrm{DS}}}{d},$$

is proportional to the ratio of the DS period and the specimen thickness. If $d_{\mathrm{DS}}/d \ll 1$, F_{inh} is much smaller than the stray energy (15) of a homogeneously deformed sample, which is proportional to the sample volume. In this case, the onset of the DS in AFM is promoted by the reduction of the stray energy which counterbalances the energy increase related to the inhomogeneous strain distribution. In the opposite case of a thin sample, $d_{\mathrm{DS}} \sim d$, the formation of the DS is unfavourable and the sample is single domain below the Néel point.

4. Domain structure in an external magnetic field

The approach developed is especially helpful for the description of the variation of macroscopic parameters under the action of an external magnetic field. For the sake of definiteness, let us consider a thin plate of a collinear AFM with the plane normal parallel to the principal crystal axis. A good example of such an AFM is $\mathrm{CoCl_2}$ (the symmetry group is $\mathrm{D_{3d}}$), underdoped $\mathrm{YBa_2Cu_3O_{6+\mathit{x}}}$ at $x \leqslant 0.3$ (the symmetry group is $\mathrm{D_{4h}}$) or cubic $\mathrm{KNiF_3}$ and $\mathrm{KCoF_3}$ single crystals. The corresponding contribution to the stray energy (15) is

$$F_{\mathrm{stray}} = L^2 d\{\tfrac{1}{2}c_{11}[\langle u_{xx}\rangle^2 + \langle u_{yy}\rangle^2] + c_{12}\langle u_{xx}\rangle\langle u_{yy}\rangle + 2c_{66}\langle u_{xy}\rangle^2\}, \tag{19}$$

where the z-axis is oriented along the plate normal.

The multidomain state of AFM in an external magnetic field $\boldsymbol{H}$ can be considered as a mixture of different phases with chemical potentials μ_k (neglecting the small demagnetization effects), which can be expressed as

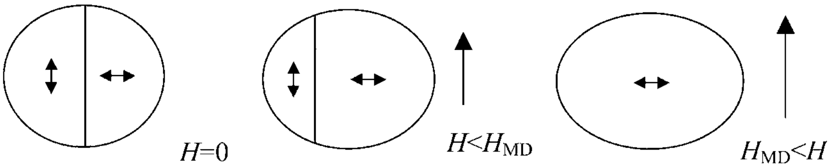

Figure 4. Smearing of the spin-flop transition for tetragonal AFM. In zero magnetic field the two domains (depicted by two-sided arrows) are equally represented. Below the field of the ‘monodomainization’, $H < H_{\rm MD}$, the fraction of unfavourable domains diminishes; the whole sample is slightly distorted. At $H_{\rm MD} < H$ the sample is single domain and only rotation of AFM moments is possible.

$$\mu_k = E_{\rm an} + \frac{M_0}{2H_E}(\boldsymbol{H}\cdot\boldsymbol{l}_k)^2 + \hat{u}_k\hat{\hat{\lambda}}_{\rm me}\boldsymbol{l}_k\otimes\boldsymbol{l}_k + \frac{1}{2}\hat{u}_k\hat{\hat{c}}\hat{u}_k. \tag{20}$$

Here, $E_{\rm an}$ is the magnetic anisotropy energy, M_0 is the saturation magnetization, $2H_E$ is the magnitude of the spin-flip field of exchange nature, $\boldsymbol{l}_k$ and $\hat{u}_k$ are the vector of the AFM and the spontaneous magnetostriction tensor, respectively, in the kth domain ($k = 1, 2, 3$ for $\rm CoCl_2$ and $k = 1, 2$ for $\rm YBa_2Cu_3O_{6+\mathit{x}}$, $\rm KNiF_3$, and $\rm KCoF_3$), and $\hat{\hat{\lambda}}_{\rm me}$ is the rank-4 tensor of the magnetoelastic coefficient. In the case of movable domain walls the volume fraction of the kth domain ξ_k is an internal thermodynamic variable related to μ_k, that can be found by minimizing the free energy:

$$\Phi = L^2 d\sum_k \xi_k\mu_k + F_{\rm stray}. \tag{21}$$

The averaged strain tensor in (19) is calculated as $\langle\hat{u}\rangle = \sum_k \xi_k\hat{u}_k$.

Standard analysis of equilibrium states (for details see [27, 28]) reveals the similarity in behaviour of the magnetoelastic DS of AFM and magnetic DS of ferromagnets. If the magnetic field is applied along one of the easy axes for the AFM vector (see figure 4), the domain walls move so as to increase the fraction of the ‘favourable’ domains (with AFM vectors perpendicular to the field direction) at the expense of the ‘unfavourable’ domains (with AFM vectors parallel to the field direction). So, instead of a drastic spin-flop transition one should observe smooth variation of the macroscopic properties (magnetization, magnetostriction) due to redistribution of the DS. One example was reported in [7] for the magnetostriction of $\rm CoCl_2$. In this process the chemical potentials of all the domains are kept equal and the effective magnetic field remains zero. Unfavourable domains are swept out of the sample when the external magnetic field attains the value

$$|\boldsymbol{H}| = H_{\rm MD} \equiv \lambda_{\rm eff}M_0\sqrt{\frac{H_E M_0}{c_{\rm eff}}} = u^{(0)}\sqrt{\frac{H_E c_{\rm eff}}{M_0}}, \tag{22}$$

where $\lambda_{\rm eff}$ and $c_{\rm eff}$ are certain combinations of magnetoelastic and elastic constants that should be calculated taking account of the concrete symmetry of the crystal. The quantity $u^{(0)} = (\lambda_{\rm eff}M_0^2/c_{\rm eff})$ in (22) stands for the absolute value of the local spontaneous shear strain. The domain fraction depends quadratically on H and saturates or vanishes at $H = H_{\rm MD}$. For example, for $\rm YBa_2Cu_3O_{6+\mathit{x}}$, $\rm KNiF_3$, or $\rm KCoF_3$,

$$\xi_{1,2} = \frac{1}{2}\left(1 \pm \frac{H^2}{H_{\rm MD}^2}\right). \tag{23}$$

The characteristic field of monodomainization H_{MD} is temperature dependent due to the temperature dependence of $M_0(T)$. Taking into account that $H_E \propto M_0(T)$, one obtains from (22) that

$$H_{\mathrm{MD}} \propto M_0^2(T). \tag{24}$$

Below the field of monodomainization the average shear strain

$$\langle u^{(0)} \rangle = \frac{\lambda_{\mathrm{eff}} M_0^2}{c_{\mathrm{eff}}} \left(\frac{H}{H_{\mathrm{MD}}} \right)^2 = u_0 \left(\frac{H}{H_{\mathrm{MD}}} \right)^2 \tag{25}$$

follows the quadratic field dependence normalized by the factor of the monodomainization field value. Thus, the low-field dependence of any macroscopic property which depends upon the relative fraction of the elastic domains should follow the law of 'corresponding states', i.e., should coincide for different substances in the reduced coordinates H/H_{MD} for the case $H \leqslant H_{\mathrm{MD}}$.

To make an appropriate comparison with the experimental data, one should take into account the field-induced isomorphous contribution to the observed macroscopic value. For example, in the case of magnetostriction, an observed elongation of the sample in the direction $\boldsymbol{N}$ relative to the crystallographic axes can be expressed as

$$\frac{\delta \ell}{\ell} = \boldsymbol{N}(\langle \hat{u}_{\mathrm{shear}} \rangle + \hat{u}_{\mathrm{iso}})\boldsymbol{N}, \tag{26}$$

where $\hat{u}_{\mathrm{iso}}$ is the isomorphous striction:

$$\hat{u}_{\mathrm{iso}} \propto \left(\frac{H}{H_E} \right)^2. \tag{27}$$

The first term in (26) is significant at low field values, below the monodomainization field $H < H_{\mathrm{MD}}$; the second one governs the field dependence in the monodomain phase up to the Néel point.

5. Discussion

The theoretical model developed allows us to describe appropriately a great deal of experimental data. In table 1 we compare characteristic fields of monodomainization calculated from the formula (22) and experimentally established values for different substances. In $\mathrm{KNiF_3}$ and $\mathrm{KCoF_3}$, Safa and Tanner [20] observed directly a reversible displacement of the domain wall under the action of the magnetic field. The wall displacement x which could be associated with the domain fraction was found to increase as

$$x \propto \frac{H^2 - H_{\mathrm{th}}^2}{H_{\mathrm{cr}}^2 - H_{\mathrm{th}}^2}, \tag{28}$$

and the experimentally established values of the critical and threshold fields were, respectively, $H_{\mathrm{cr}} = 1.65$ T and $H_{\mathrm{th}} = 0.3$ T for $\mathrm{KCoF_3}$ and $H_{\mathrm{cr}} = 0.4$ T and $H_{\mathrm{th}} = 0.1$ T for $\mathrm{KNiF_3}$. The critical field H_{cr} is associated in table 1 with the field of monodomainization H_{MD}. The threshold field at which the domain walls start to move depends upon the activation energy and could not be estimated in the present model.

Analogous observations of the S-type domain structure in NiO were made by Yamada [4]. The characteristic field is evaluated as the field at which one system of the domains disappears.

Observations of redistribution of the DS in $\mathrm{CoCl_2}$ AFM were made indirectly, on the basis of magnetostriction versus magnetic field dependence, by Ryabchenko and co-workers [24]. In this case, the monodomainization field is determined from the saturation of the low-field magnetostriction.

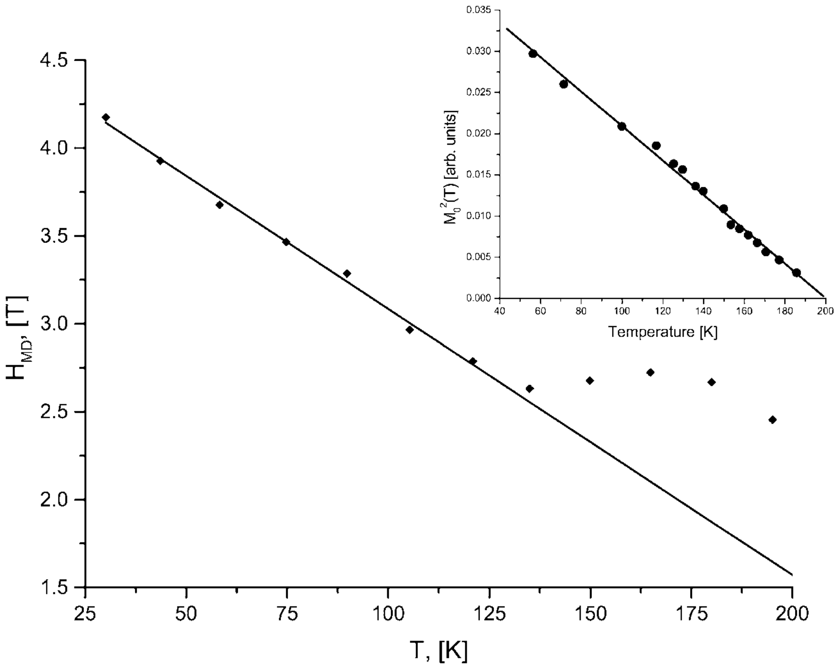

Figure 5. The temperature dependence of the 'monodomainization' field H_{MD} for $\mathrm{YBa_2Cu_3O_{6.3}}$, constructed using the data from [31, 32]. The inset shows a plot of $M_0^2(T)$ calculated according to the data from [9].

Table 1. Characteristic values and monodomainization fields for different AFM. The quantity $\hat{u}^{(0)}$ denotes the magnetostriction; M_0 is the magnetization value.

AFM	$u^{(0)}$	M_0 (kG)	H_E (T)	c_{eff} (GPa)	$H_{\mathrm{MD}}^{\mathrm{theor}}$ (T)	$H_{\mathrm{MD}}^{\mathrm{exp}}$ (T)	References
$\mathrm{KCoF_3}$	3×10^{-3}	0.5	200	30	2.0	1.65	[20, 44, 45]
$\mathrm{KNiF_3}$	$\sim3\times10^{-5}$	0.3	280	30	0.5	0.4	[20, 44, 45]
$\mathrm{CoCl_2}$	4×10^{-4}	0.32	3.2	34.7	0.33	0.2–0.3	[7, 24, 29]
NiO	9×10^{-5}	1.02	1000	109	0.66	0.7–0.8	[4, 23, 46, 47]

Table 1 shows a rather good agreement between the calculated and experimentally observed values of the monodomainization field, which corroborates the magnetoelastic origin of the DS.

Further confirmation of the model can be found by applying it to the description of the field dependence of the magnetoresistance of the $\mathrm{YBa_2Cu_3O_{6.3}}$ compound over a wide temperature range. Magnetoresistance is a macroscopic characteristic; it is described by a symmetric second-rank tensor. Therefore, its field dependence is the same as that for the magnetostrictive strain tensor. We have processed the data kindly provided by Lavrov (and published in [31, 32]) in the following way: first, we subtracted a high-field background (27) of exchange nature and, then, we approximated the magnetoresistance $\rho_{xx}-\rho_{yy}\equiv\Delta\rho$ using a formula analogous to (25):

$$\frac{\Delta\rho(H)}{\rho_0}=\frac{\Delta\rho(0)}{\rho_0}\left(\frac{H}{H_{\mathrm{MD}}}\right)^2. \tag{29}$$

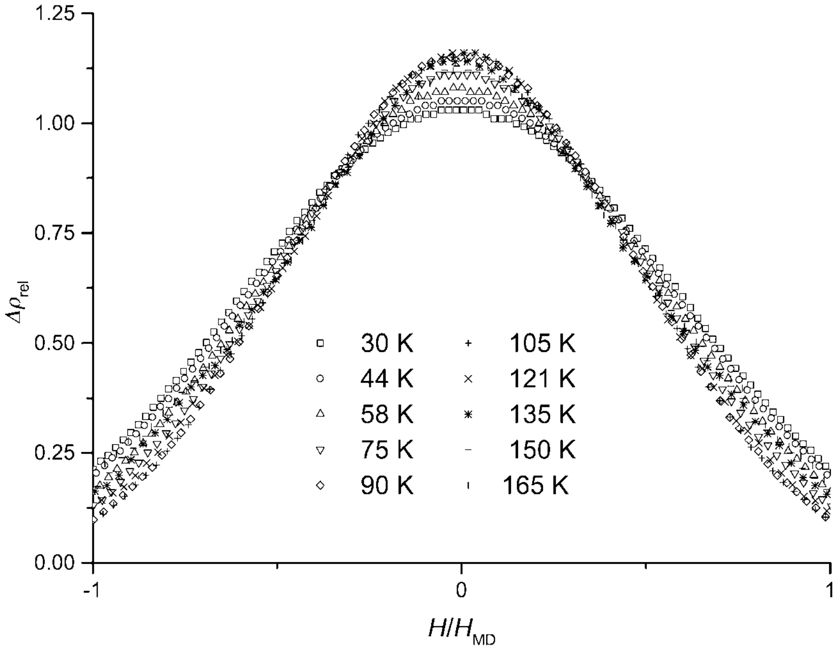

Figure 6. The dependence of the longitudinal component of the magnetoresistance of $YBa_2Cu_3O_{6.3}$ on the field $\boldsymbol{H} \parallel \boldsymbol{a}$ and temperature, representing the law of 'corresponding states'. This graph was constructed using the data from [31, 32] plotted in reduced coordinates: $\Delta\rho_{rel} = \Delta\rho/\Delta\rho_0$, H/H_{MD}.

Figure 5 shows the temperature dependence of the thus-calculated field of monodomainization H_{MD}. The inset gives the plot of $M_0^2(T)$ calculated according to the data from [9]. It can be clearly seen that below 150 K the monodomainization field H_{MD} and $M_0^2(T)$ follow the same linear temperature dependence, in accordance with theoretical prediction (24). Deviations from the linear dependence observed at higher temperatures could be explained by the influence of defects. The defects pin the domain walls and diminish the fraction of the mobile domains participating in the redistribution of the DS. At low temperature the defects are immobile and thus give rise to a systematic error (which is the same for all temperatures) in the monodomainization field compared with the ideal theoretical value (24). At higher temperatures the mobility of the defects can be high enough to allow relaxation processes. In this case a fraction of the pinned domain wall can be essential and the characteristic field of monodomainization would be defined by reorientation processes, i.e., by the value of the spin-flop transition field. Anyway, change of the temperature dependence of the monodomainization field indicates change of the mechanism that governs the formation of the equilibrium DS.

Figure 6 presents the field dependence of the magnetoresistance in the reduced coordinates $\Delta\rho(H)/\Delta\rho(0)$, H/H_{MD}, which illustrates the law of 'corresponding states' (25) for the same compound. All the curves, over a wide temperature range (below 150 K), are very close to each other. Consequently, they are governed by the same mechanism.

6. Conclusions

The main results of the paper can be formulated as follows:

(1) The equilibrium DS that arises in the course of the phase transition into the AFM state results from the finite-size effects closely related to the properties of the sample surface. The absolutely rigid surface produces the imaginary 'incompatibility elastic charges' whose long-range field contributes to the energy of the sample, the corresponding contribution being proportional to the sample volume and thus providing the twinning effect.

(2) The contribution from the inhomogeneous distribution of the strain below the phase transition point is proportional to the DS period and in the case of large samples is vanishingly small.

(3) The elastic stray energy is the reason for the onset of the equilibrium DS in the easy-plane collinear AFM. The domain distribution can be regulated in a reversible way by the external magnetic field.

(4) The low-field dependence of the macroscopic parameters should be the same for different samples if compared in the reduced coordinates H/H_{MD} (the law of 'corresponding states').

Acknowledgments

The authors are grateful to Professors V G Barýakhtar, M A Ivanov, V I Marchenko and S M Ryabchenko for numerous and very useful discussions on the problem of possible mechanisms of DS formation in AFM. HG would like to thank A A Malyshenko for financial and technical support and especially thanks Professor J Kirschner for making it possible to use the facilities of MPI in Halle (Saale) and Dr M Nyvlt for numerous discussions, sound criticism and help in manuscript preparation. The work of VML was partially supported by the Swiss National Science Foundation under SCOPES-project 7UKPJ062150.00/1.

References

[1] Néel L 1953 *Proc. Int. Conf. on Theoretical Physics Science Council of Japan, Tokyo* **1954** 701

[2] Baruchel J, Schlenker M and Roth W L 1977 *J. Appl. Phys.* **48** 5

[3] Saito S, Miura M and Kurosawa K 1980 *J. Phys. C: Solid State Phys.* **13** 1513

[4] Yamada T, Saito S and Shimomura Y 1966 *J. Phys. Soc. Japan* **21** 672

[5] Spooner F J and Vernon M W 1969 *J. Mater. Sci.* **4** 734

[6] Stout J W and Hsu C-S 1971 *17th Annual Conf. on Magnetism and Magnetic Materials* (Chicago, IL: AIP)

[7] Wilkinson M K, Cable J W, Wollan E O and Koehler W C 1959 *Phys. Rev.* **113** 497

[8] Eremenko V V and Kharchenko N F 1984 *Sov. Sci. Rev.* A **5** 1

[9] Burlet P, Henry J Y and Regnault L P 1998 *Physica* C **296** 205

[10] Janossy A, Simon F, Feher T, Rockenbauer A, Korecz L, Chen C, Chowdhury A J S and Hodby J W 1999 *Phys. Rev.* B **59** 1176

[11] Hosoya S and Ando M 1971 *Phys. Rev. Lett.* **26** 321

[12] Nakotte H, Bruck E, de Boer F R, Svoboda P, Tuan N C, Havela L, Sechovsky V and Robinson R A 1993 *J. Appl. Phys.* **73** 6551

[13] Szuszkiewicz W, Hennion B, Jouanne M, Morhange J F, Dynowska E, Janik E, Wojtowicz T, Zielinski M and Furdyna J K 1998 *Acta Phys. Pol.* A **94** 583

[14] Barýakhtar V G, Bogdanov A N and Yablonskii D A 1988 *Sov. Phys.–Usp.* **31** 810

[15] Bogdanov A N and Dragunov I E 1998 *Sov. J. Low Temp.* **24** 852

[16] Farztdinov M M 1964 *Sov. Phys.–Usp.* **7** 853

[17] Li Y Y 1956 *Phys. Rev.* **101** 1450

[18] Eremenko V V, Kharchenko N F and Beliy L I 1979 *J. Appl. Phys.* **50** 7751

[19] Baruchel J, de Camargo P C, Klein H, Mazzaro I, Nogues J and de Oliveira A 2001 *J. Phys. D: Appl. Phys.* **34** A114

[20] Safa M and Tanner B K 1978 *Phil. Mag.* B **37** 739

[21] Tanner B K 1979 *Contemp. Phys.* **20** 187

[22] Schlenker M and Baruchel J 1978 *J. Appl. Phys.* **49** 1996
[23] Roth W L 1960 *J. Appl. Phys.* **31** 2000
[24] Kalita V M, Lozenko A F, Ryabchenko S M and Trotsenko P A 1998 *Ukr. Fiz. Zh.* **43** 1469 (in Ukrainian)
[25] Olson G B and Cohen M 1986 *Dislocation Theory of Martensitic Transformations (Dislocations in Solids vol 7)* ed F R N Nabarro (Amsterdam: North-Holland)
[26] Roytburd A L 1998 *J. Appl. Phys.* **83** 228
[27] Gomonaj E V and Loktev V M 1999 *Sov. J. Low Temp.* **25** 699
[28] Gomonaj E V and Loktev V M 2000 *Acta Phys. Pol.* A **97** 459
[29] Kalita V M, Lozenko A F and Ryabchenko S M 2000 *Sov. J. Low Temp.* **26** 671
[30] Amitin E B, Baikalov A G, Blinov A G, Boyarskii L A, Dikovskii V Y, Zdanov K R, Kamenev M Y, Kozeeva L P and Shelkovnikov A P 1999 *Pis. Eksp. Teor. Fiz.* **70** 350 (in Russian)
[31] Ando Y, Lavrov A N and Segawa K 2000 *Physica* C **341–8** 1535 (cond-mat/0004135)
[32] Lavrov A N, Kameneva M Y and Kozeeva L P 1998 *Phys. Rev. Lett.* **81** 5636
[33] Ando Y, Lavrov A N and Segawa K 1999 *Phys. Rev. Lett.* **83** 2813
[34] Watson G M, Gibbs D, Lander G H, Gaulin B D, Matzke H and Ellis W 2000 *Phys. Rev.* B **61** 8966
[35] Watson G M, Gibbs D, Lander G H, Gaulin B D, Matzke H and Ellis W 1996 *Phys. Rev. Lett.* **77** 751
[36] Wolfram T, Dewames R E, Hall W F and Palmberg P W 1971 *Surf. Sci.* **28** 45
[37] Gutjahr-Löser T, Sander D and Kirschner J 2000 *J. Magn. Magn. Mater.* **220** L1
[38] Carlotti G, Socino G, Hu A, Xia H and Jiang S S 1994 *J. Appl. Phys.* **75** 3081
[39] Carlotti G, Gubbiotti G, Socino G, Pareti L and Turilli G 1997 *J. Magn. Magn. Mater.* **165** 424
[40] Kléman M and Schlenker M 1972 *J. Appl. Phys.* **43** 3184
[41] Teodosiu C 1982 *Elastic Models of Crystal Defects* (Berlin: Springer) p 352
[42] Marchenko V I and Parshin A Y 1980 *Sov. Phys.–JETP* **52** (in Russian)
[43] de Wit R 1960 *Solid State Physics* vol 10 (New York: Academic) p 249
[44] Aleksiejuk M and Kraska D 1975 *Phys. Status Solidi* a **31** K65
[45] Pari G, Jaya S M and Asokamni R 1994 *Phys. Rev.* B **50** 8156
[46] Plessis P, Tonder S J and Alberts L 1971 *Solid State Physics* vol 4 (New York: Academic) p 1983
[47] Plessis P, Tonder S J and Alberts L 1971 *Solid State Physics* vol 4 (New York: Academic) p 2565